Earth and Planetary Science Letters 325–326 (2012) 27–38

Contents lists available at SciVerse ScienceDirect

Earth and Planetary Science Letters

journal homepage: www.elsevier.com/locate/epsl

The onset of the lunar cataclysm as recorded in its ancient crater populations

Simone Marchi [a,b,c,*], William F. Bottke [b], David A. Kring [c], Alessandro Morbidelli [a]

[a] Laboratoire Lagrange, Université de Nice Sophia-Antipolis, CNRS, Observatoire de la Côte d'Azur, France
[b] Center for Lunar Origin & Evolution, SwRI, Boulder, CO, USA
[c] Center for Lunar Science & Exploration, USRA — Lunar and Planetary Institute, Houston, TX, USA

ARTICLE INFO

Article history:
Received 21 November 2011
Received in revised form 16 January 2012
Accepted 18 January 2012
Available online 22 February 2012

Editor: T.M. Harrison

Keywords:
the Moon
lunar cataclysm
solar system evolution
South Pole-Aitken basin

ABSTRACT

The earliest bombardment history of the Moon potentially provides powerful constraints for solar system evolution models. A major uncertainty, however, is how much of this history is actually recorded in lunar craters. For example, some argue that most ancient lunar craters and basins were produced by a declining bombardment of leftover planetesimals produced by terrestrial planet formation processes. Others believe that most lunar craters and large basins were formed in a narrow time interval between 3.8 and 4.0 Ga, the so-called lunar cataclysm. In the light of recent improvements in our understanding of early solar system evolution, it is possible that the contributions from both scenarios could be represented in the lunar crater record. If so, when did the declining bombardment end and the lunar cataclysm begin?

Here we show, using new counts of 15–150 km diameter craters on the most ancient lunar terrains, that the craters found on or near Nectaris basin appear to have been created by projectiles hitting twice as fast as those that made the oldest craters on various Pre-Nectarian-era terrains. This dramatic velocity increase is consistent with the existence of a lunar cataclysm and potentially with a late reconfiguration of giant planet orbits, which may have strongly modified the source of lunar impactors. This work also suggests that the lunar cataclysm may have started near the formation time of Nectaris basin. This possibility implies that South Pole-Aitken basin (SPA), the largest lunar basin and one of the oldest by superposition, was not created during the cataclysm. This view is strengthened by our interpretation that a substantial fraction of ancient craters on SPA were made by low velocity impactors. Finally, we believe these results shed new light on the impact history of the primordial Earth.

1. Introduction

The lunar cratering record is perhaps the most complete, clear, and accessible history available for the inner solar system over the last ~4.5 Gy. The spatial density of lunar craters not only provides a measure of the relative age of different surfaces, but can also help us understand the temporal evolution of the impactor flux that has struck the Earth–Moon system over time. The ultimate goals of lunar cratering studies are to determine absolute ages using a combination of sample ages and modeling work, and to glean insights into those planet formation and evolution processes that produce lunar impactors.

The interpretation of craters on the oldest lunar terrains is often divided into two broad schools of thought. The first suggests that the leftovers of planetary accretion struck the Moon after it formed, with the flux declining smoothly as the planetesimals were gradually eliminated over hundreds of Myr by collisional and dynamical processes (e.g., Wetherill, 1977). In an end-member case, the declining bombardment phase would dominate the production of lunar craters and basins (i.e., $D > 300$ km diameter craters) until at least 3.7–3.8 Ga, the formation time of the youngest basin Orientale (Hartmann, 1975; Hartmann et al., 1981; Marchi et al., 2009; Neukum and Ivanov, 1994).

The second school suggests most basins and craters formed in an impact spike or so-called lunar cataclysm (LC; Kring and Cohen, 2002; Ryder, 2002; Tera et al., 1974). While the actual length of the impact spike is a hotly debated topic, support for some kind of LC comes from the apparent clustering of impact-reset Ar–Ar ages and extensive crustal U–Pb mobilization at 3.8–3.9 Ga found within Apollo samples (Tera et al., 1974; Turner et al., 1973) and lunar meteorites (Cohen et al., 2000). Numerical modeling work also indicates it is unlikely that a conventional declining bombardment model could make large lunar basins like Imbrium and Orientale between their observed ages of 3.7–3.9 Ga (Bottke et al., 2007). In an end-member case, nearly all lunar craters and basins would be made by the LC within a window of time that includes 3.7–3.9 Ga (Ryder, 2002). A possible trigger for the LC could be the putative late migration of the giant planets (Gomes et al., 2005).

Both schools are difficult to prove or reject because few of the available lunar samples with solid ages can be definitively linked to specific impact features or terrains (Norman et al., 2010; Stöffler and Ryder, 2001). For example, the observed paucity of impact-reset

* Corresponding author at: Laboratoire Lagrange, Université de Nice Sophia-Antipolis, CNRS, Observatoire de la Côte d'Azur, France.
E-mail address: marchi@oca.eu (S. Marchi).

0012-821X/$ – see front matter © 2012 Elsevier B.V. All rights reserved.
doi:10.1016/j.epsl.2012.01.021

argon ages older than 3.9 Ga may be due to an over-reliance on samples taken from the vicinity of Imbrium basin (and its ejecta) rather than a true indication that the LC took place (Chapman et al., 2007; Hartmann et al., 2007; Haskin et al., 1998). Still, it is possible that an either-or choice here may be the wrong question to ask.

In this paper, we argue that both schools should contribute at some level to the lunar cratering record. This outcome is predicted by numerical modeling work; late stage terrestrial planet formation models show a declining bombardment of leftover planetesimals is almost inevitable in the inner solar system (e.g., Bottke et al., 2007; Morbidelli et al., 2001), while late giant planet migration models may well extract comets and asteroids out of their stable reservoirs hundreds of millions of years after the terrestrial planets and Moon have formed. Thus, in a unified model, the oldest craters and basins would come from a declining bombardment phase, while somewhat younger ones would be derived from a LC of limited extent. If true, we might expect a change in the impactor populations between the declining bombardment and LC eras. In turn, this would translate into a change in the crater size-frequency distributions (SFDs) between the oldest lunar terrains and those occurring near the LC event. The question is whether this signal can be found in the existing crater data. In this respect, it is important to point out that key differences in the crater SFDs between the ancient lunar highlands and the much younger post-mare terrains have already been identified by Strom et al. (2005). Their work showed that the oldest lunar terrains have a crater SFD that looks like the impactors were extracted from the main asteroid belt by a size-independent process (e.g., perhaps sweeping resonances driven by planet migration; Gomes et al., 2005; Minton and Malhotra, 2009; Strom et al., 2005). The post-mare terrains, however, have a crater SFD that looks like it came from the present-day Earth-crossing object population, with the projectiles pulled out of the main belt via a size-dependent process (e.g., the Yarkovsky thermal drift forces combined with dynamical resonances; Morbidelli and Vokrouhlický, 2003).

A final note of caution is warranted here. While the similarity between the existing main belt and ancient lunar terrains identified by Strom et al. (2005) may indeed represent evidence for the LC, we find it at least remotely conceivable that a comparable signature could come from a long-lived leftover planetesimal population gradually transitioning into a population dominated by Earth-crossing objects delivered from the main belt. For this model to explain the Strom et al. (2005) observations, it would need to do the following: (i) the population itself would need to collisionally evolve into the same shape as the main belt size-frequency distribution, and (ii) it would need to decay much more slowly than suggested by existing dynamical models (e.g., Bottke et al., 2007).

In fact, if a LC took place, and early crater records were not obliterated by this process, the lunar crater record should show two transitions. The first would be between the earliest population of impactors, presumably a combination of leftover planetesimals from terrestrial planet accretion and early ejected members of small body reservoirs, and a later LC population potentially produced by the dynamical destabilization of those small body reservoirs. The second would be between LC projectiles and the same near-Earth object (NEO) population that appears to have dominated the production of lunar craters over the last ~3 Ga. Our work here focuses on ancient lunar crater populations in the hope that a careful analysis of recent high quality lunar data might reveal the nature of the putative first transition, i.e. between the early and LC impactor populations. Here we show, using new crater counts of some of the oldest lunar terrains, that a fingerprint of this transition does exist, and that it supports the lunar cataclysm hypothesis.

2. Terrain selection

Crater identification and counts were performed on the digital terrain model (DTM) produced by the Lunar Orbiter Laser Altimeter (LOLA) (Smith et al., 2010) on board the Lunar Reconnaissance Orbiter (LRO) spacecraft. The resolution of the DTM was 64-pixel-per-degree. During the crater identification processes, we also compared LOLA DTM to comparable resolution shaded relief maps produced by Lunar Orbiter and Clementine (data available at http://www.mapaplanet.org/explorer/moon.html).

Crater counting was performed with a semi-automated code according to the following steps: i) the regions of interest were divided in sub-regions of about 10×10 deg^2; ii) within each sub-region, craters (identified by visual inspection) were registered by mouse clicking on 5 points over their rims; iii) the 5 selected points are used to perform a circular best fit, returning the center position and the diameter of the craters; iv) all identified craters are saved on an ASCII file for post processing. Crater size frequency distributions are built selecting craters which lay within given regions of interest. In this work we focus on craters larger than about 15 km, because smaller craters may be severely affected by secondary craters (i.e. formed by fragment ejected by other craters; Wilhelms, 1987; Wilhelms et al., 1978) and thus they can strongly alter subsequent analysis.

An important issue was to assess how our crater counts relate to those that existed in the literature (e.g., Head et al., 2010; Neukum and Ivanov, 1994; Strom et al., 2005; Wilhelms, 1987). The main problem in performing such a comparison arises from the choice of the terrains. In most cases, published crater counts are not accompanied by a detailed map showing the boundaries of the terrains used. The choice of the terrains is indeed crucial, in particular for the oldest terrains that may suffer from episodes of partial resurfacing (e.g., via formation of nearby basins and volcanic eruptions). Nevertheless, in order to validate our crater identification and diameter estimate, we performed several tests with well-known individual craters and crater SFDs over some large basins from Wilhelms (1987). We also compared our counts with the global catalog of craters >20 km by Head et al. (2010). For the former, those tests indicate that the discrepancy in our crater diameter estimates is of the order of 1– 3% for individual craters. We also found that our crater SFDs are in fairly good agreement (within the error bars) for terrains near or inside a number of lunar basins (e.g., Apollo, Birkhoff). For the latter, comparisons over similar regions showed that the crater counts were within the counting Poissonian error bars. Although it is sometimes unclear on what terrains the crater counts were made that appear in the literature, we explicitly identify our regions of interest in the following sections.

To determine if there is a transition between an older declining bombardment crater population, or what we will refer to here as the "early population", and a younger LC crater population, or what we refer to here as a "late population", we examined three sets of terrains. The first two correspond to some of the most ancient terrains on the Moon, where the putative early and late populations are likely to be combined together in some fashion. The first region analyzed corresponds to a wide portion of the Pre-Nectarian terrains on the northern far side. The second region includes Pre-Nectarian terrains on the floor of the largest impact basin on the Moon, South Pole-Aitken (SPA) basin. For our third region, we wanted to examine lunar terrains that formed well after the oldest terrains, yet one that still was older than the transition to the present day Earth-crossing population. Our hypothesis is that this younger terrain would hopefully be dominated by the late population. We also wanted a large area that would allow us to avoid small number crater statistics and produce a broad range of crater diameters. Our choice was to examine the region near the 860 km diameter Nectaris basin, roughly the twelfth youngest basin on the Moon and a benchmark used to define time periods on the Moon (Wilhelms, 1987). Nectaris is also the closest large basin to the Apollo 16 landing site. If Apollo 16 samples were dominated by ejecta from this basin, its radiometric age could be as young as 3.92 Ga (Stöffler and Ryder, 2001), although impact lithologies with still speculative provenance have been found with ages of 4.1–4.2 Ga (Norman et al., 2010). In our work, we examined the

Nectaris basin floor, its rim regions, and a portion of its ejecta blanket deposited prior to the Imbrium basin-forming event.

Surfaces designated for crater counting in these terrains were selected using a multi-step approach. First, macro-areas were identified according to geological mapping methods (Wilhelms, 1987). In doing so, only macro-areas corresponding to pre-Nectarian and Nectarian terrains were considered. Pre-Nectarian terrains are defined as those terrains emplaced prior to the Nectaris basin-forming event. Therefore pre-Nectarian terrains mix regions of different ages which often also correspond to multiple geological units. A similar conclusion also applies to Nectarian terrains. In this respect, we point out that terrain boundaries indicated by (Wilhelms, 1987) are often due to a basin's ejecta blankets. Therefore, ejecta blankets of Nectarian-era basins (e.g., Nectaris, Moscoviense, Mendeleev) are also tagged as Nectarian terrains. This, however, applies only to the ejecta layer, which decreases in depth for increasing distance from the basin's rim (e.g., McGetchin et al., 1973; see on-line material). Depending on the thickness of the deposits, previously existing craters may be detectable below a thin ejecta layer. Therefore the crater count for Nectarian terrains might not always correspond to truly Nectarian ages. Thus, a second, more specific selection is required in order to have surfaces representative of a single geologic unit and a unique age. We describe our specific selections below from youngest to oldest in terms of crater density.

2.1. Nectaris Basin

The identification of Nectaris terrains coeval with its formation are challenging. Nearly half of the basin floor has been filled by mare that post-dates the basin's formation (Mare Nectaris). Moreover, about 75% of the continuous ejecta have been covered by subsequent ejecta from the Imbrium basin. Here we examine two Nectaris basin terrains (NBT hereinafter). The first one (NBT1) is restricted to the Nectarian part of the basin floor and extends only marginally outside the nominal rim of the basin. This minimizes contamination by pre-existing craters (see Fig. 1). The second selection (NBT2) encompasses NB1 terrains and extends over a wider portion of basin ejecta (out to roughly two radii from the basin center) where crater obliteration from Nectaris debris may have been effective at resetting the crater counting clock. We carefully avoided secondary craters and pre-Nectarian craters, consistent with USGS 1:1,000,000 geological map series (Milton, 1968; Rowan, 1971; Elston, 1972; Stuart-Alexander and Tabor, 1972; Hodges, 1973).

The resulting crater SFDs are shown in Fig. 2, both in terms of cumulative and R-value distributions (see figure caption for the definition of R-values). The two distributions overlap over a wide range of diameters. Subtle differences exist for craters with diameter $D>70$ km. The lower spatial density of large craters in NBT2 is interpreted to be solely from small number count statistics. Therefore, we argue the largest area of NBT2 (simply indicated by NBT in the rest of the paper) offers the least biased crater population.

2.2. South Pole-Aitken Basin

South Pole-Aitken basin is 2400×2100 km in diameter, and its floor is one of the oldest terrains on the Moon. In fact, using several arguments, including stratigraphy and secondary craters superposition, Wilhelms (1987) presented a chronological relationship of pre-Nectarian terrains, with SPA presented as the very oldest basin. The age of the basin itself, however, may differ from its floor, which has experienced several episodes of alteration that postdate its formation. Some of the SPA floor modification events include the formation of several large basins (e.g., Planck, Poincare, Apollo), mare eruptions inside some of those internal basins, SPA's rim cut by large external basins like Keeler–Heaviside and Australe, and the emplacement of ejecta from distant basins like Orientale. Despite these factors, a significant portion of SPA's floor is still preserved (see plate 6A–6B of Wilhelms, 1987) and can be used to estimate the crater SFD recorded since the underlying terrains were created. To overcome the above issues, we counted craters on multiple terrains in order to ensure a robust determination of the oldest crater SFD found. In this manner, we potentially avoid issues that come up with cryptomare emplacement and resurfacing episodes, since they are unlikely to affect all of our sub-terrains in exactly the same fashion. Here we discuss what we can actually count on SPA terrains (SPAT hereinafter).

The first selection (SPAT1) is based on the pre-Nectarian terrains of plate 6A–6B of Wilhelms (1987) which are inside the rim of SPA basin. We excluded mare from Apollo basin (not indicated in the above plates, see Fig. 3). Note that the white-coded terrains of Wilhelms' plates excluded from SPAT1 have different origins; they range from maria to basin ejecta and crater floors. Basin ejecta are mainly from Schrödinger (inside SPA) and Orientale (outside SPA).

The second selection (SPAT2) includes several large young craters excluded from SPAT1 (Fig. 3). Their exclusion may artificially reduce the crater counts for SPA basin in the $D>100$ km range. The crater SFDs found on SPAT1 and SPAT2 also include Planck, Poincare and Apollo basins. The third selection (SPAT3) also includes Schrödinger, Antoniadi and Amundsen–Ganswindt basins and their ejecta (Fig. 3). Finally the fourth selection (SPAT4) excludes from SPAT3 the cryptomare region in the central portion of the SPA basin floor.

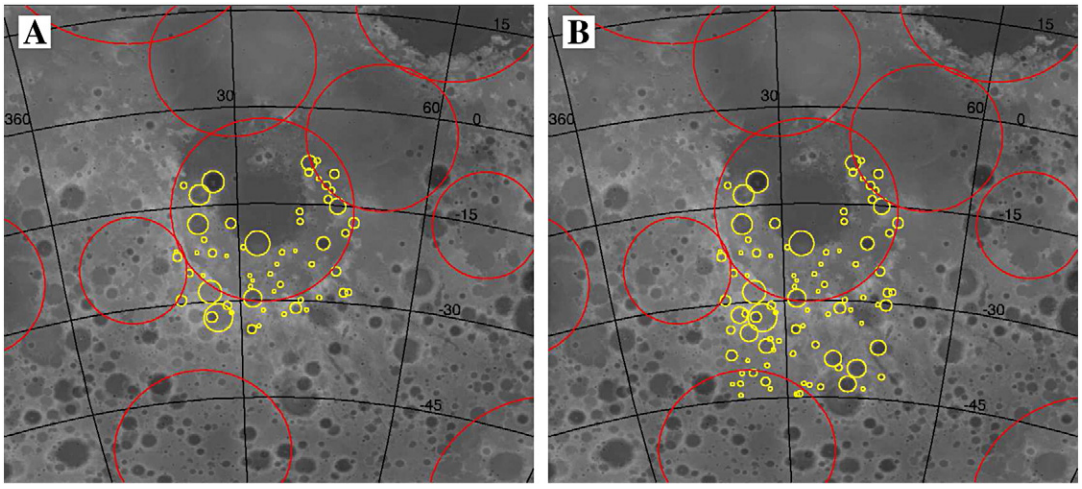

Fig. 1. The map (LOLA DTM) shows the Nectaris basin terrains used in this work. A: NB1 terrains ($0.48\cdot10^6$ km^2, 57 craters). B: NB2 terrains ($0.74\cdot10^6$ km^2, 92 craters). Yellow circles indicate the rims of counted craters, while red circles indicate the rims of impact basis (Wilhelms, 1987).

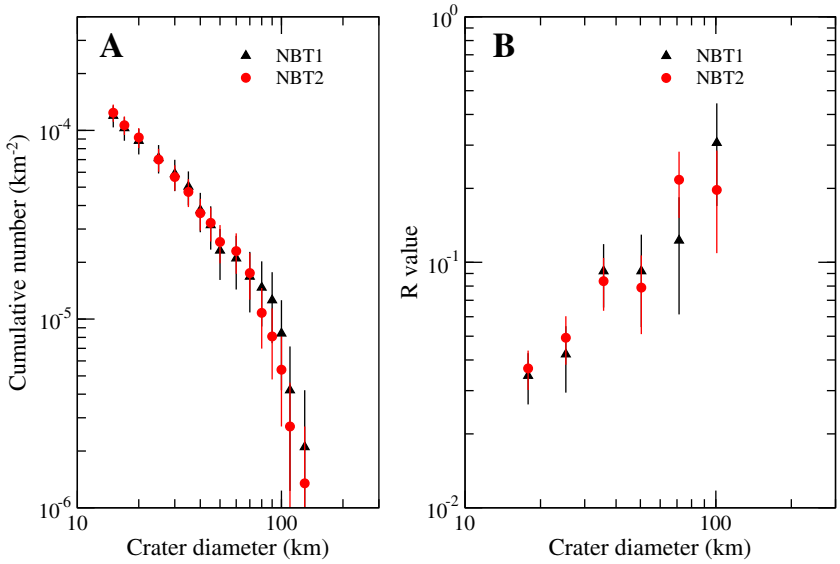

Fig. 2. Comparison between Nectaris basin NBT1 and NBT2 crater SFDs. Panel A) shows the cumulative values per unit surface while panel B) the relative values (R-values). R-values are computed by cumulative crater SFD normalized to a power law D^{-2} (Crater Analysis Techniques Working Group et al., 1979). Error bars correspond to the square root of the count (Poisson statistics) for each bin.

The region covered by cryptomare is defined according to Gibson and Jolliff (2011).

The resulting crater SFDs are shown in Fig. 4. The four distributions shown here are in overall good agreement, confirming our assessment that the crater SFD of SPA is robust. The main difference between SPAT1 and SPAT2 is in the $100<D<200$ km range and may be caused by small number statistics. SPAT2 and SPAT3 differ slightly for $D<50$ km, though they are in good agreement for $D<50$ km. SPAT3's deficit of smaller craters may be due to erasure of smaller craters in SPAT3 by subsequent basin formation (e.g., Schrödinger, Antoniadi, Amundsen–Ganswindt, and Schrödinger–Zeeman). Finally, SPAT3 and SPAT4 are basically identical, which implies that the cryptomare region did not significantly modify our crater counts over most of the diameter ranges discussed in this paper. It is possible, though, that cryptomare may have obliterated some of the smallest craters considered here. For this reason in subsequent analysis of SPAT crater SFDs, we limit our consideration to $D>20$ km.

Our interpretation is that SPAT2 (simply indicated as SPAT in the rest of the paper) is the most representative of the SPA basin floor, and therefore it has been used in the remainder of our analysis.

2.3. Pre-Nectarian terrains outside SPA basin

Several pre-Nectarian terrains (PNTs) are located outside of the SPA basin (see Plate 6A–6B of Wilhelms, 1987). They are largely made up of basin floors and ejecta blankets, yet they encompass a wide range of geological properties. They have also been affected by subsequent basin formation and distal ejecta. An interesting question is whether specific PNT terrains were formed after the SPA basin, were reset by the SPA basin and therefore have the same age as the

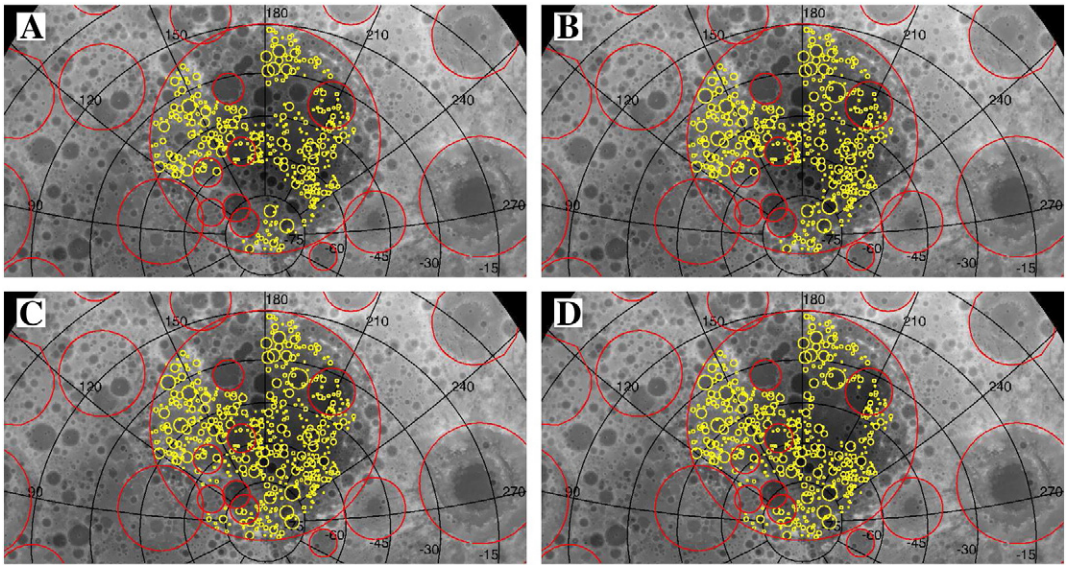

Fig. 3. The maps (LOLA DTMs) show the SPA basin terrains used in this work. A: SPAT1 terrains ($2.09\cdot10^6$ km^2, 389 craters). B: SPAT2 terrains ($2.41\cdot10^6$ km^2, 429 craters). C: SPAT3 terrains ($3.16\cdot10^6$ km^2, 497 craters). D: SPAT4 terrains ($2.86\cdot10^6$ km^2, 458 craters). Yellow circles indicate the rims of counted craters, while red circles indicate the rims of impact basis (Wilhelms, 1987).

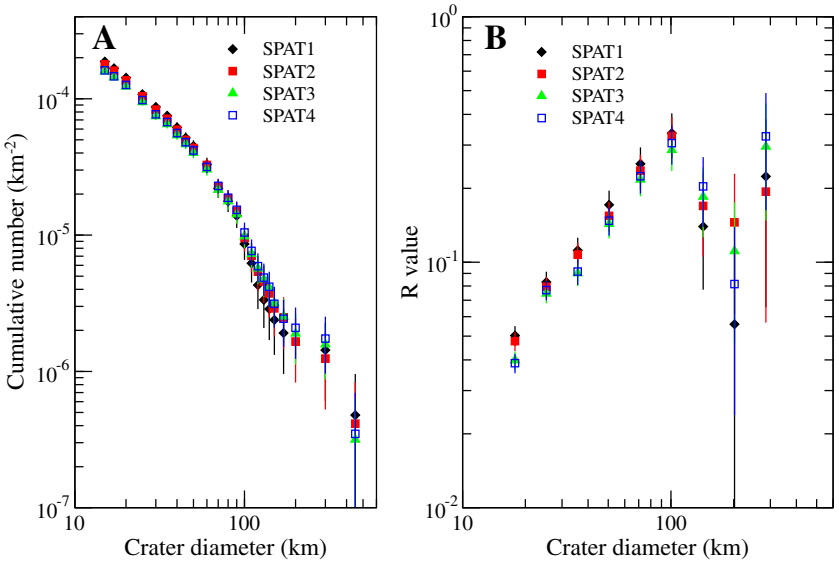

Fig. 4. Comparison among cumulative (A) and relative-value (B) crater SFDs within the South Pole-Aitken basin. See text for further details.

SPA basin, or could actually be older than the SPA basin. We take no stand on this issue, but the chronological relationships of some basins to the SPA basin are admittedly weak (e.g., Lorentz, Birkhoff and Coulomb–Sarton). This issue warrants a closer examination in the future using imagery data from LRO.

To make sure our results were not affected by concerns over precise geologic boundaries, we divided PNTs into several sectors and treated them separately. The first selection (PNT1) is considered the largest part of the northern Pre-Nectarian terrains (see plate 6B of Wilhelms, 1987; see Fig. 5). These terrains appear to be less affected by basin formation than any other pre-Nectarian terrains on the lunar far side outside of the rim of SPA basin. The second selection (PNT2) is similar to PNT1, but includes some young large craters (see Section 2.2). Because the resulting crater SFDs show negligible differences (see Fig. 6), we choose to use PNT2.

To address the possibility of contamination of PNT2 by ejecta from SPA, we also examined PNT3 and PNT4. Both correspond to PNT2 terrains that have been limited to angular distances from the center of SPA by $>90°$ and $>110°$, respectively. For similar reasons, we investigated two very old units close to SPA's rim. PNT5 is near the center of the far side and is exterior to the Keeler–Heaviside basin. PNT6 is on the nearside and is comprised of the region between Mutus–Vlacq, Australe and SPA basins (Fig. 5).

The resulting crater SFDs are shown in Fig. 6. The general agreement among PNT2 through PNT6 indicates that there are no discernible systematic effects of secondary cratering with regards to increasing distance from SPA's rim or that any other basin (e.g., Imbrium, Orientale). The spread in crater spatial densities, particularly for PNT5 and PNT6, is likely due to limited crater counting areas and small number statistics. The selected terrains are also at different distances from the Imbrium basin, which is known to have produced large secondary craters (Wilhelms, 1987). Thus, the overall stability of the crater SFDs also rule out a significant contamination of secondary craters from Imbrium basin. The rest of the discussion below will use crater SFDs from PNT2 (indicated for simplicity by PNT).

Fig. 6 also shows crater counts from the lunar highlands that were reported in Strom et al. (2005). While some small differences exist because we used different crater bin sizes than Strom et al., our PNT2 terrains essentially agree with their SFDs for $30<D<200$ km. The small discrepancies that do exist, namely for $D<30$ km and $D>200$ km, are likely caused by the different terrain choices. In particular, the Strom et al. (2005) crater SFD was constructed using the nearside highlands for $D<180$ km and the whole lunar surface for $D>180$ km.

3. Comparative analysis of the observed crater SFDs

Fig. 7 shows our measured crater SFDs for our three terrains. At first glance, several things stand out. First, while PNT has a higher surface crater density than SPAT for $15<D<60$ km, both are within error bars within the range $60<D<150$ km. Second, for $D>300$ km, PNT is higher than SPAT by a factor of ~2, although the statistics are poor at these crater sizes. Third, the crater density on NBT is lower than both SPAT and PNT, as expected given its presumed relatively younger age.

Perhaps the most intriguing observation, however, is that all of the crater SFDs are well reproduced by two-sloped distributions up to $D=150$ km (see Fig. 8). The slope of a crater SFD is defined as $\Delta log(N)/\Delta log(D)$, where N is the cumulative density of craters. We found these slopes by plotting the crater data for each terrain in log-log space and then fitting lines (or power laws) to the small and large craters over specific size ranges. The intersection between the derived slopes for the small and large craters was defined as D_{elbow}. By calculating the slopes in this manner, we hope to minimize any issues generated by the stochastic nature of cratering itself, namely that crater SFDs do not always perfectly reproduce the shape of the impactor SFD.

Our crater ranges for small and large craters were carefully chosen for each terrain, partly to maximize the amount of crater data available for each fit, but also to exclude the intermediate regions where the distributions pass from one slope to the other. For small D and large D, we selected [15, 50] km, [70, 100] km for NBT; [20, 50] km, [60, 150] km for SPAT; and [15, 40] km, [60, 150] km for PNT. Note that SPAT craters smaller than 20 km have been excluded because their number may have been affected by cryptomare (see Section 2.2). Computing the weighted mean values for the slopes from PNT, SPAT and NBT together, we found best fits for -1.25 ± 0.03 over small crater diameters and -2.6 ± 0.1 over larger ones, respectively.

We conclude that the three terrains share remarkably similar slopes for their small and large crater populations. With this said, we found that D_{elbow} varies substantially from one distribution to another, with the most heavily cratered terrains have D_{elbow} at smaller sizes than those on less cratered, younger terrains. Thus, the crater

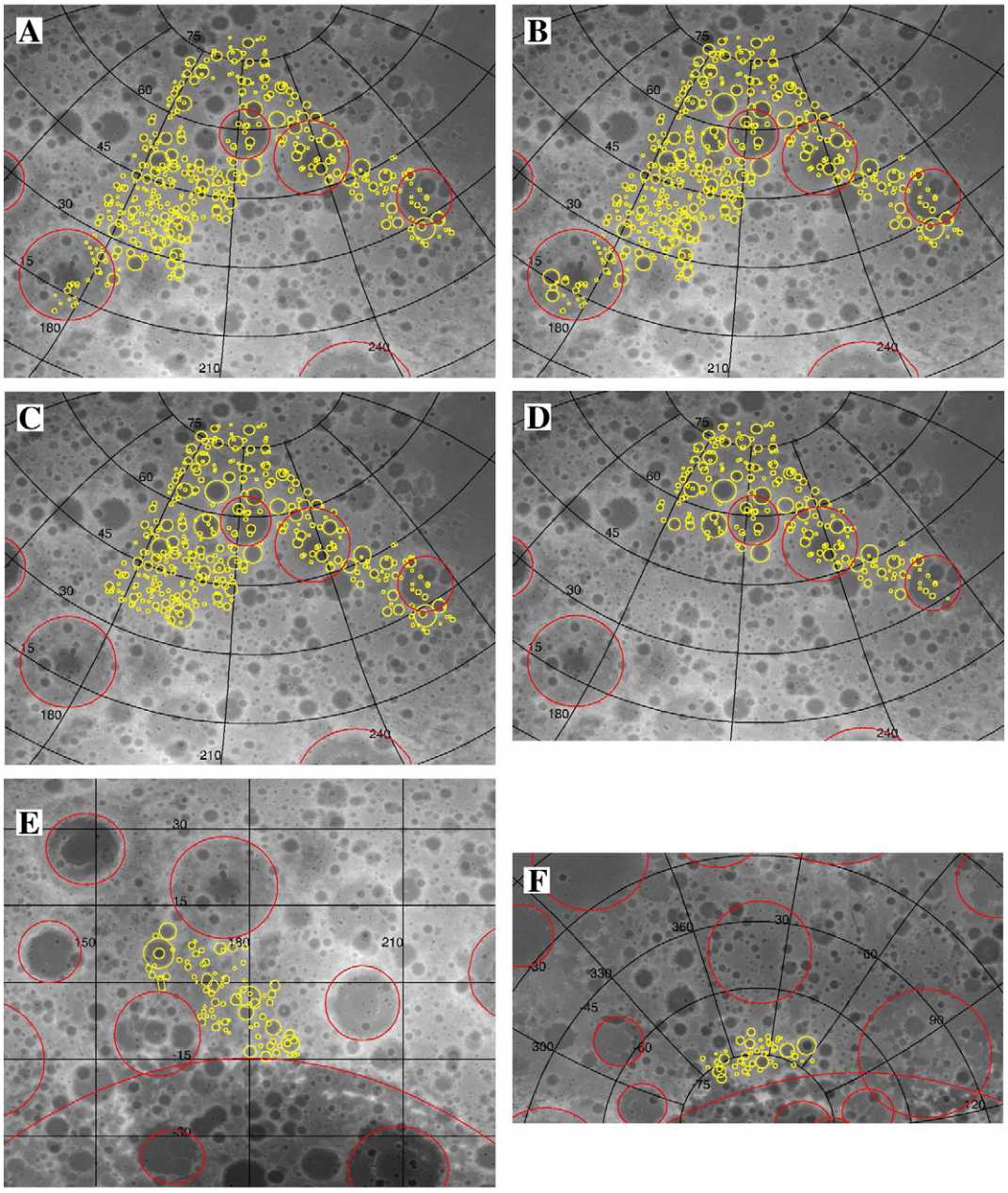

Fig. 5. The maps (LOLA DTMs) show the pre-Nectarian terrains used in this work. A: PNT1 terrains ($1.52 \cdot 10^6$ km^2, 382 craters). B: PNT2 terrains ($1.75 \cdot 10^6$ km^2, 415 craters). C: PNT3 terrains ($1.37 \cdot 10^6$ km^2, 344 craters). D: PNT4 terrains ($0.91 \cdot 10^6$ km^2, 188 craters). E: PNT5 terrains ($0.35 \cdot 10^6$ km^2, 86 craters). F: PNT6 terrains ($0.49 \cdot 10^6$ km^2, 121 craters). Yellow circles indicate the rims of counted craters, while red circles indicate the rims of impact basis (Wilhelms, 1987).

SFDs are alike in particular ways but very different in other ways. We found the differences suggestive enough to pursue them further in the following section.

4. Are the crater SFDs on PNT and SPAT statistically different?

In order to quantify the differences between the observed crater SFDs and their D_{elbow} values, we turned to Monte Carlo simulations of how these cratered terrains were plausibly created. For each trial, we created random craters drawn from a source function that duplicated the observed cumulative crater SFD for each terrain. Once the observed number of craters was created, we used the procedure above to measure the slopes for small and large D. The elbow position D_{elbow} was then determined by calculating the intercept of the corresponding two best fit lines. This was done 1000 times for each crater SFD.

The resulting distributions of D_{elbow} values were then used as a measure of how statistical fluctuations in the creation of these crater SFDs modify the observed D_{elbow} value. Our work indicates that the D_{elbow} 68.2% (1σ) level of confidence intervals for PNT, SPAT, NBT are [37.9, 54.9] km, [56.6, 66.2] km and [59.8, 75.0] km, respectively. Similarly, the median values of D_{elbow} are 47.7 km, 61.9 km, 68.3 km. We find it interesting that the $\sim 1\sigma$ intervals reported above are disjoint. This means that a single crater production function (with a single D_{elbow} value) is extremely unlikely to have made all three of our crater SFDs and can be ruled out at the $\sim 2\sigma$ level.

An alternative way to understand this result is the following. Assume that a single production function is responsible for the crater SFDs on PNT and SPAT. This would imply that the difference in counts for $D > 20$ km craters is due to the terrains having different ages. Then, multiply the crater SFD on SPAT by a factor 1.27, so that the

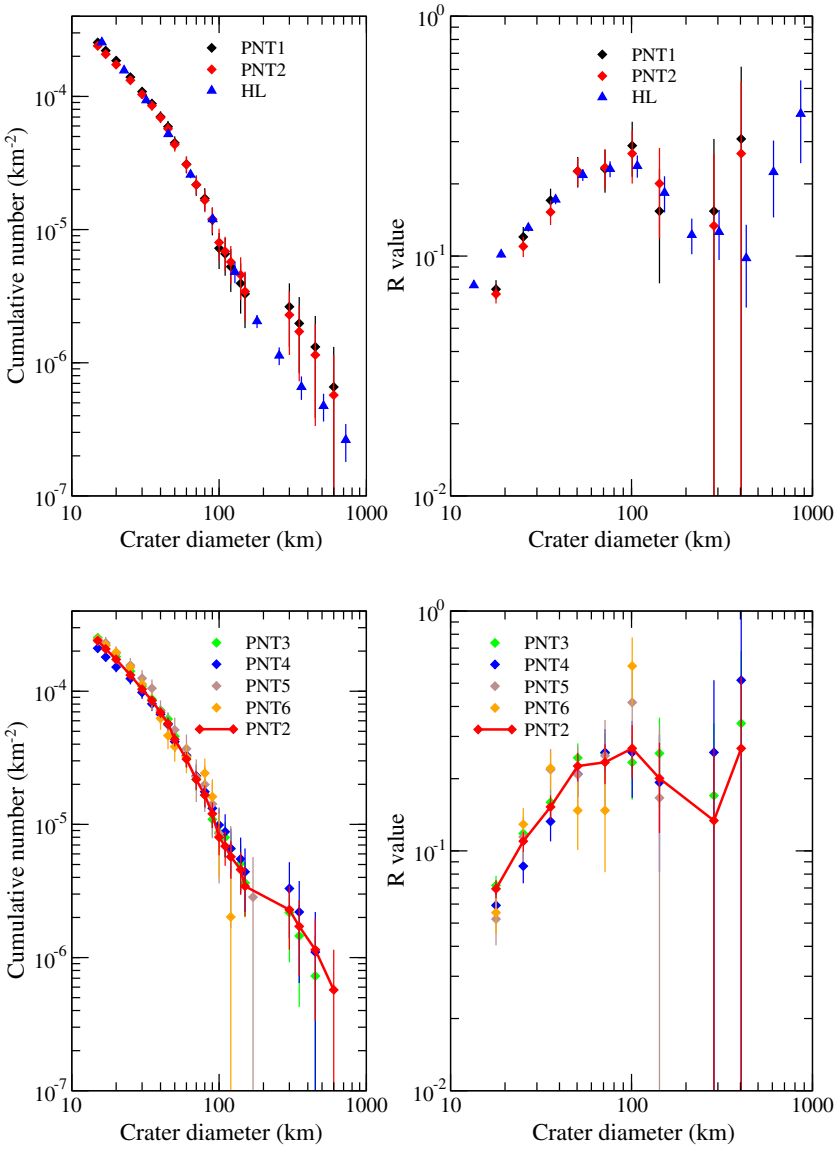

Fig. 6. Comparsion among the several Pre-Nectarian terrains investigated. Top panels: Comparison between PNT1 and PNT2 crater SFDs. The lunar highland crater SFD of Strom et al. (2005) is also reported (HL). Bottom panels: Comparison among PNT2 through PNT6 crater SFDs.

two cumulative SFDs coincide at $D=20$ km. This change causes the crater SFDs to separate by more than their respective error bars in the range $50<D<90$ km. In particular, the re-scaled crater SFD for SPAT, once multiplied by the appropriate area, would predict that 73 ± 8.5 craters with $D>60$ km formed on PNT. Instead, the observed number of $D>60$ km craters observed on PNT is 54 ± 7.3. The possibility that 54 ± 7.3 craters formed if 73 ± 8.5 were expected can also be ruled out at the 2.2σ level.

We conclude from this that the D_{elbow} differences between the two oldest terrains, PNT and SPAT, are unlikely to be statistical fluctuations. Using similar arguments, the same is true for the younger NBT as well. Thus, the observation that D_{elbow} values grow larger as one moves from older terrains like PNT to younger terrains like SPAT and NBT appears robust.

5. On the possible sources of the differences among crater SFDs

5.1. Crater saturation

One concern about our interpretation above involves the potential influence of crater saturation. Saturation takes place when the density of craters on a given surface exceeds some threshold value, such that newly-formed craters erase pre-existing ones (Gault, 1970). When this occurs, the surface density of craters cannot continue to increase with time, though the shape of the crater SFD can potentially be influenced by newly-formed craters. Given that the crater SFDs on PNT and SPAT overlap in the range $60<D<150$ km, a possible explanation might be that these terrains reached crater saturation at these sizes.

To investigate whether our terrains were influenced by saturation, we first examined whether some regions of the Moon were more densely cratered than PNT. Along these lines, we counted craters on the Pre-Nectarian Al-Khwarizmi-King terrain (AKKT) as defined by Wilhelms (1987). We found that this terrain, though smaller than PNT, has crater densities that are 30% higher than PNT between $25<D<60$ km. It also appears to have a similar D_{elbow} value to PNT, though small numbers crater statistics beyond $D>60$ km prevent us from considering this a robust result (see on-line material). As a follow-up, we examined crater statistics from Head et al. (2010), who was first to use the LOLA database to count $D>20$ km craters on the Moon. Their work indicates there are several lunar regions with higher crater densities than PNT (i.e., some are 1.5× higher, with a $D>20$ km crater density of 0.28 km^{-2} vs. 0.17 km^{-2} for our

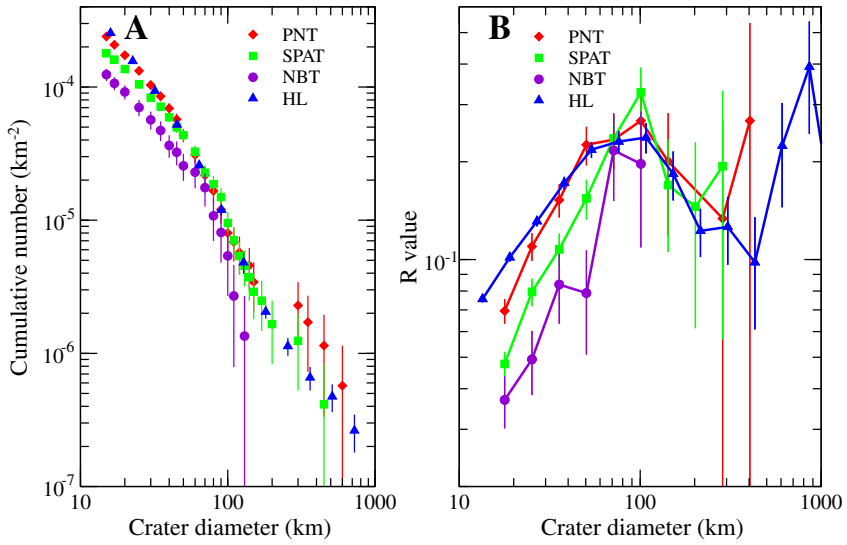

Fig. 7. Crater size-frequency distributions of the selected terrains. The distributions reported here correspond to our final terrain choice: NBT, SPAT, PNT stand for NBT2, SPAT2 and PNT2 of previous plots. A: Comparison of the cumulative crater SFDs. The lunar highland crater SFD of Strom et al. (2005) is also reported (HL). B: Relative value distributions. Both panels A and B show that PNT and SPAT crater SFDs overlap in the interval $60<D<150$ km, while they differ for $15<D<60$ km. NBT is less cratered (i.e., younger) than both PNT and SPAT.

PNT). Together, these results demonstrate that lunar crater density can locally exceed PNT values, thereby implying that PNT (and SPAT and NBT) are not saturated. This conclusion is in agreement with previous observational studies (Strom, 1977; Strom et al., 2005).

Second, we decided to investigate crater saturation using an improved version of the crater formation/evolution model by Bottke and Chapman (2006). Our code simulates the random formation of craters on a square surface according to a input production function. Craters are defined by their rims, and when more than 70% of a crater's rim is removed by overlapping craters, the crater is removed from the count. The code tracks the progress of the crater SFD throughout the simulation. In this manner, the overall approach of our code mimics those described in the literature (Chapman and McKinnon, 1986; Richardson, 2009; Woronow, 1985).

Crater obliteration in the code is modeled by considering that, when a new crater (D) is formed, it destroys a portion of the rim of a crater underneath (D_u), but only if $D_n > D_u/f$, where $D_n = kD$. In these expressions f and k ($f,k \geq 1$) are parameters that simulate the obliteration processes: f takes into account the capability of small craters to erase the rims of larger ones; while k increases the effective area of erasing, as for instance in the presence of significant ejecta blanket and/or seismic shaking. Note that for the crater production functions investigated in this paper, f and k are essentially interchangeable. Thus, for a given f, increasing k would produce the same results as keeping k fixed and increasing f. While the parameters f,k are unknown a priori, they can potentially be calibrated using benchmark data. Here we set these parameters using one of the best examples of saturated terrain known in the existing lunar data, namely the $\sim 10^6$ craters counted in the Sinus Medii region (Gault, 1970). Fig. 9 (upper panels) shows the best fit achieved with $f \sim 9$, $k \sim 1$ (in agreement with previous runs by Bottke and Chapman, 2006). As far as we know, no other crater evolution code has tested their results against this or any comparable data set, yet this is crucial if one is to avoid non-uniqueness issues in chosen model parameters.

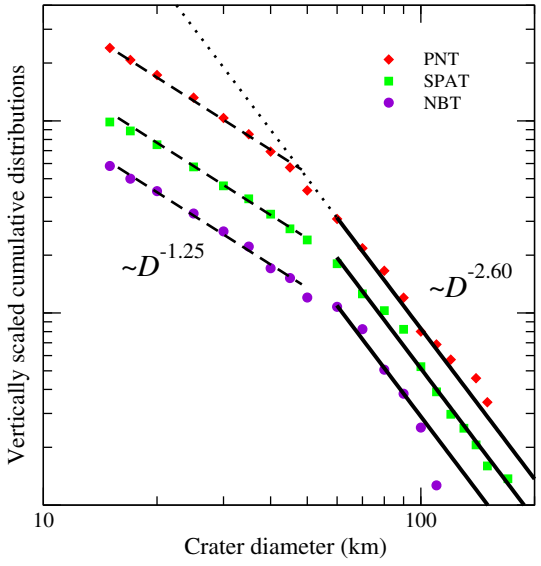

Fig. 8. Comparison of PNT, SPAT and NBT crater SFDs. The distributions have been vertically rescaled for a better comparison. The dashed lines approximate the observed crater SFDs for small D. These lines are parallel, thus they show that PNT, SPAT and NBT have the same slopes. A similar conclusion applies for large D (see solid lines).

Using the same parameters used to fit Sinus Medii craters, we simulated crater formation on PNT (see Fig. 9, bottom panels). Our results suggest that PNT is not expected to be saturated. With this said, however, the crater SFDs of PNT and Sinus Medii have different size ranges, so we cannot rule out that a different choice of f,k could apply for PNT. For example, Head et al. (2010) found that the formation of Orientale basin partially erased $D > 20$ km craters up to two radii from the basin's center. In our code, this would translate into $k \sim 1.5$. This is a likely upper limit, with smaller craters perhaps having more difficulty erasing nearby craters than basins, but even the application of $k = 1.5$ to all crater sizes does not allow PNT to enter into saturation (see on-line material). We underline that our finding that PNT is not saturated while the much younger Sinus Medii is saturated is indeed possible given the different crater size range investigated on these terrains.

It is interesting to note that our results are discordant with Richardson (2009), who found the Strom et al. (2005) crater SFD on the lunar highlands was indeed saturated. This conclusion was reached using a different model of crater erasure than ours; it performs the same basic functions as our code but it also includes regolith displacements by seismic shaking and the burial of craters via ejecta blanketing. We take no issue with their results, but merely point out that the predictions of saturation in either code depends on model parameters that may be difficult to constrain given the current state of knowledge. Regardless, even if the lunar highlands and PNT were in saturation, both

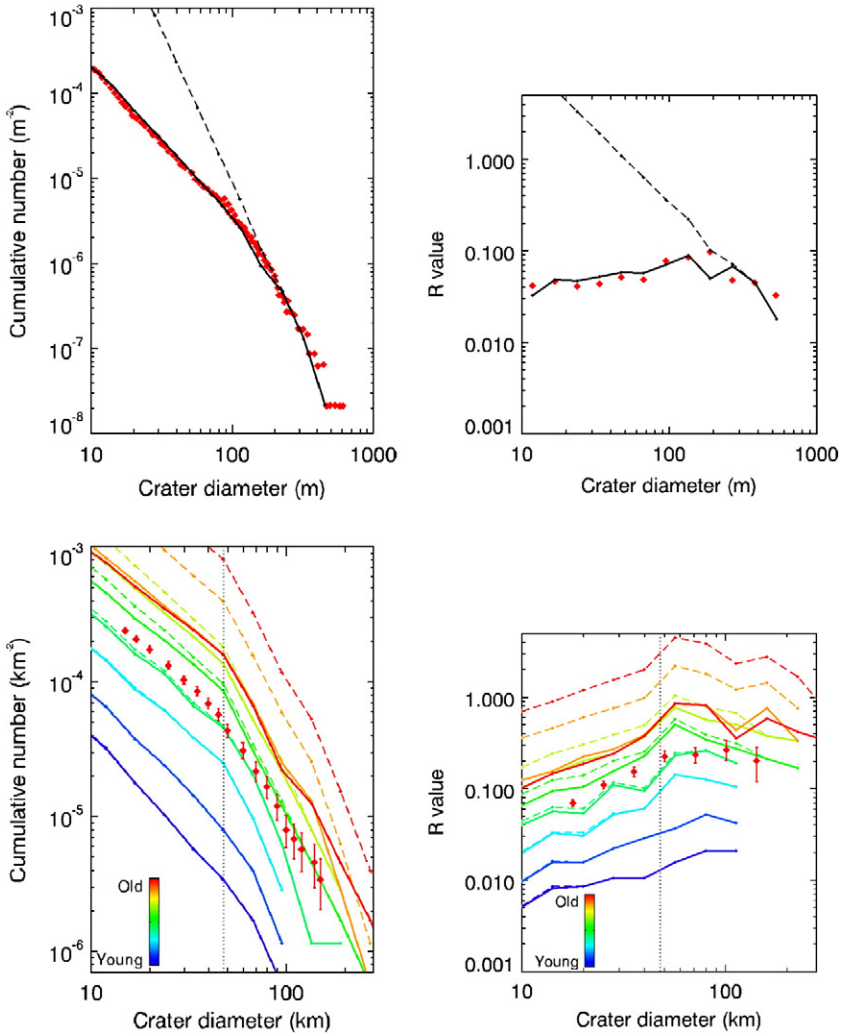

Fig. 9. Upper panels: The plot report the crater SFD for the saturated lunar Sinus Medii region (Gault, 1970). The SFD is shown in a cumulative fashion in the left panel and in an R-plot in the right panel. The lines correspond to the best fit, achieved for $f=9$ and $k=1$. The dashed lines indicated the production population (i.e., no crater obliteration), while the solid curves correspond to the population of crater left on the surface (i.e., taking into account obliteration processes). Bottom panels: The plots show the evolution of the crater record for $f=9$, $k=1$ and a two-sloped production function having $q=-1.25$ for $D<D_{\rm elbow}$ and $q=-2.6$ for $D>D_{\rm elbow}$, where $D_{\rm elbow}=47.7$ km (best value for PNT). The position of the elbow is marked by the vertical dashed line. The curves are color-coded according to the total number of impacts received, from blue (less cratered, younger surface) to red (more cratered, older surface). Dashed curves indicate the production functions, while solid ones indicate the crater SFDs of the retained craters. The red dots with error bars show the observed crater SFD on PNT.

codes agree with the findings of Chapman and McKinnon (1986), who showed that it would not affect the shape of this particular crater SFD over the size range of interest (see Fig. 9).[1] Thus, even if PNT were saturated, its crater SFD could still be compared with SPAT and NBT to investigate pre- and post-LC evolution.

Taken together, these results indicate that crater saturation cannot be the explanation of the intriguing similarities and differences between the crater SFDs on PNT, SPAT, and NBT. Something else is likely afoot.

5.2. Impactor SFD and target properties

Another potential way to explain the observed differences in crater SFDs between PNT, SPAT and NBT is that the shape of impactor SFD changed with time. We find this plausible, but the subtle nature of the changes needed makes us believe that this is an unlikely way to explain observations.

For example, as shown by Strom et al. (2005), the impactor SFD that made craters on the lunar highlands also fits PNT (see Fig. 7) and is a reasonable match for the current main belt asteroid SFD. Numerical models indicate that the main belt has experienced extensive collisional evolution (Bottke et al., 2005), and that a population starting with main belt-like initial conditions, perhaps common among inner solar system planetesimal populations, quickly evolves toward an equilibrium distribution that has the same shape as today's main belt SFD. To get substantial differences away from this kind of equilibrium, some parameter(s) need to change in a major way (e.g., a large breakup event takes place, a new population is added to the system, etc.). These kinds of events, however, have to be perfectly tuned to effectively make a two-sloped SFD shift to larger sizes. In all of the collision evolution models we have run to date, we have yet to see such behavior in any runs.

Similarly, contributions from populations having different SFDs cannot be ruled out, but they would need to be perfectly tuned to explain observations (i.e., similar to the main belt SFD, only shifted in

[1] Note that saturation behaves in substantial different ways depending on the slope of the crater SFD. For crater SFDs having slopes shallower than power law −2, the saturated crater SFD keep its original shape. For slopes steeper than −2, the saturated crater SFD gets a constant slope equal to −2. This explains why, in the case of Sinus Medii, saturation introduced a clear change in the slope of the crater SFD, while the same would not happen to PNT.

every size domain, or a population with physical parameters that allows their craters at every size to look like a shifted main belt SFD). This conclusion may make it unlikely for lunar craters to have a major contribution of cometary impactors, unless they can fit the above criteria. As a side note, we point out that the highly siderophile element signatures of lunar samples appear to indicate that comets did not play a major role in the Moon's early bombardment phase (Kring and Cohen, 2002).

Target properties also play a role in the cratering process, and potentially may affect the shape of the crater SFDs. The size of a crater made by a projectile depends on many factors, including target structure (hard rock vs loose material), density, and mechanical strength. The craters discussed in this paper form in the gravity regime, thus, mechanical strength is not expected to play an important role. Similarly, target density should be similar from place to place on the Moon, and it also has a weak influence on crater size ($\sim\rho^{-0.3}$). In fact, depending on how this parameter was manipulated, it could even produce the opposite effect what is needed to explain observations (i.e., if all other parameters are constant, higher density terrains such as the floor of SPA may produce smaller craters than low density terrains like PNT). Finally, according to crater scaling relationships, a change in target structure should also produce a change in the slope of the crater SFD. This is not observed. Indeed the nearly identical slopes of the crater SFDs of our terrains and the consistent shift in elbow positions from older to younger terrains appear to us to be strong constraints that are difficult to explain using the effects described above.

Thus, while we agree that some ad-hoc combination of the above parameters might be able to reproduce observations, we would also argue that those conditions will most likely run the gamut from unlikely to unphysical.

6. Discussion and implications

In the previous sections, we argued that the crater SFDs of PNT, SPAT, and NBT likely reflect the impactors that formed them, and that their shapes are remarkably similar to one another. Their main difference is that the location of D_{elbow} increases as we move from older to younger terrains. What could cause such a change? Some precedent for our situation can be found in Strom and Neukum (1988). They report that the most ancient crater SFDs found on Mercury, the Moon, and Mars have main belt-like shapes, but those on Mercury and Mars are shifted to larger and smaller diameters, respectively, compared those found in the lunar highlands. One way to do this is to assume the projectiles hit Mercury and Mars much faster and slower, respectively, than they hit the Moon (e.g., assuming the projectiles came from the main belt, Minton and Malhotra (2010) estimate they hit Mercury, the Moon, and Mars at 38.1 km/s, 18.9 km/s and 12.4 km/s, respectively). By inserting these velocities into crater-scaling relationships, they found that they could reproduce the observed crater SFD shifts on these worlds even though target properties may have also affected crater sizes (Ivanov, 2006).

Accordingly, the simplest way to explain our results is to assume that the impactor SFD remained the same in the time interval when PNT and Nectaris basin received most of their craters, but the impact velocity increased between the oldest and the youngest of the three terrains considered here (i.e., from PNT to NBT). To test this, however, we need to assess the populations hitting the Moon at different times. This is challenging because older terrains accumulate early and late impactors. In some fashion, we need to remove the late crater signatures on PNT and SPAT to explore the early ones.

Here we return to our original hypothesis, namely that the PNT and SPAT crater SFDs may have recorded, in sequence, an early and late impactor population with distinct impact velocities and D_{elbow} values. As shown in Fig. 10, we assume here that NBT was hit uniquely by an impactor population producing $D_{\mathrm{elbow}}\sim 60$ km. We will refer to this as our "late population". By subtracting NBT's contribution from PNT and SPAT, we gain a residual than can be used to estimate the nature of the "early population", or what originally struck PNT and SPAT. The fact that PNT and SPAT have the same slopes of NBT requires that the early and late populations had the same slopes. Thus, our best fits to observations show the early population had $D_{\mathrm{elbow}}\sim 45$ km rather than ~ 60 km.

Overall, the early population accounts for 48% and 32% of the craters $D\geq 15$ km observed on PNT and SPAT, respectively. The rest comes from the late population superposed on these terrains. The crater SFDs obtained by this combination of impacting populations pass through the error bars of all the data on all terrains, with one

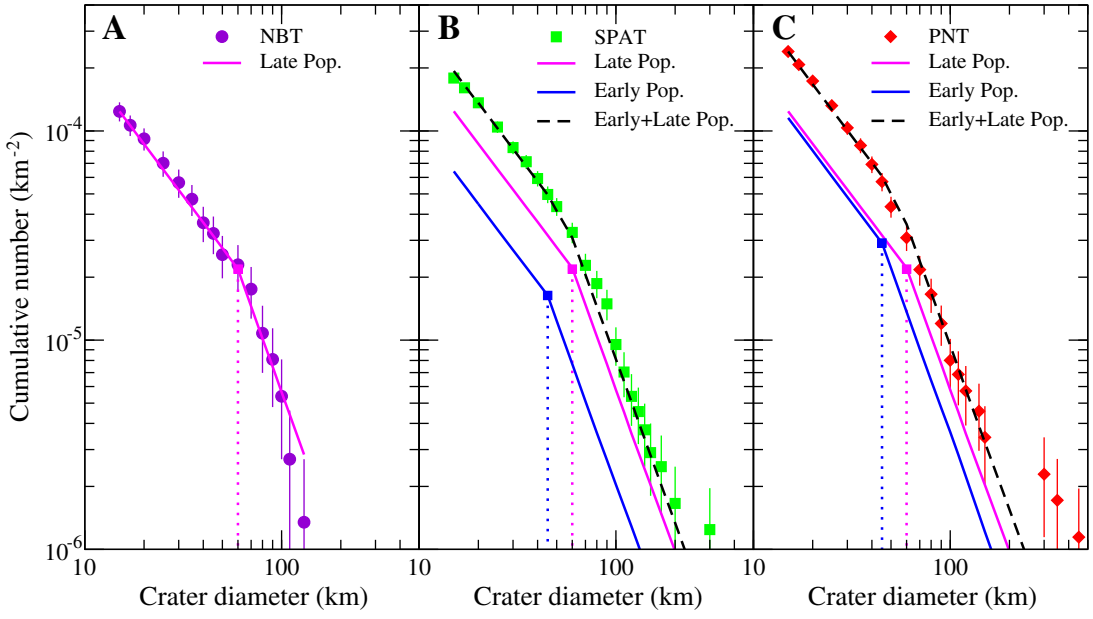

Fig. 10. Two impactor populations best fits of the observed crater SFDs. The fit is obtained assuming that each terrain records a different combination of an early and late impactor population producing $D_{\mathrm{elbow}}=45$ km and $D_{\mathrm{elbow}}=60$ km. Each panel corresponds to a different terrain as labeled. The presented model is able to explain the observed crater SFDs, and in particular, given the predicted shift in the impact velocity (and therefore in the crater size) it naturally explains why SPAT and PNT partially overlap.

exception (the data-point at $D = 90$ km on SPAT, which anomalously deviates from a smooth curve; Fig. 10B). Moreover, about 50% of the synthetic crater SFDs generated by these production functions have elbows within the corresponding 1-sigma confidence ranges for the three terrains. Considering that 68.2% is the statistical measure for a perfect fit, we believe our results are reasonable.

In the light of these findings, we conclude that the observed shift in D_{elbow} is most likely due to a variation in mean impact velocity between the early and late populations. According to Pi-group crater scaling (Schmidt and Housen, 1987), crater diameter is $\propto v^{0.44}$, where v is the impact velocity. Therefore, we estimate that the shift in D_{elbow} from the early to the late population corresponds to a factor of ~2 increase in impact velocity (i.e., $=(60/45)^{1/0.44}$). This change is significant enough to suggest important implications for the early history of the solar system.

One way to produce the observed velocity change is through late giant planet migration, which could modify the degree of dynamical excitation experienced by objects reaching or residing within the inner solar system. A numerical study of this idea (Bottke et al., submitted for publication), within the context of the so-called Nice model (Gomes et al., 2005), implies that median impact velocities on the Moon before and after giant planet migration is 9 and 21 km/s, respectively. The origin of the low velocity population may be a combination of early fugitives from the inner asteroid belt (Bottke et al., submitted for publication) and/or leftover planetesimals residing in the terrestrial planet region after the Moon's formation (Walsh et al., 2011).

Several important benchmarks in the early lunar evolution emerge from this work. First, the existence of distinct low and high impact velocity populations supports the existence of a lunar cataclysm. In particular, the high D_{elbow} of NBT suggests that these terrains record a negligible contribution of the early population, implying that Nectaris basin is close to or at the onset of the LC. This result is consistent with independent modeling work by Bottke et al. (submitted for publication) based on the overall crater density at NBT. This makes the formation age of Nectaris basin a key data point in understanding the evolution of the solar system.

Second, despite the lack of precise age measurements for our oldest terrains, it is clear that PNT and SPAT preserve a record of impacts of low velocity impacts, many which may have come before the LC from the early population. PNT was struck by nearly the same amount of pre-LC and LC impactors. This implies that PNT is very old. Our interpretation that the cataclysm started near the formation time of Nectaris basin also implies that the ancient SPA basin did not form during the LC but instead was derived from an earlier phase of lunar history. The fact that SPAT records at least some of the low velocity population provides additional support for this idea, though precise modeling is needed to better understand the very beginning of the LC. Depending on the solidification time of the lunar crust (e.g., Elkins-Tanton et al., 2011) and the early populations impact flux, both surfaces potentially recorded hundreds of My of pre-Nectarian history. This sets the stage for using crater data from ancient lunar terrains to constrain terrestrial planet formation models, at least as far as their predictions for the impact flux of leftover planetesimals.

Third, we find that PNT has as much as twice the early population recorded on its terrain than SPAT, implying a clear difference in the cratering retention age between the two terrains. While our work does not constrain whether the SPAT crater retention age is substantially younger than or similar in age to SPA basin itself, we find the latter possibility provocative and worthy of additional study. Perhaps a re-analysis of the Moon using LRO or GRAIL data will show that SPA basin is much younger than previously thought.

Finally, we find that despite its oft-used name, the lunar cataclysm only accounted for roughly half or perhaps one-third of the observed ancient crater history now recorded on the Moon. Regardless, the surprisingly and unusual impact velocity fingerprint described here potentially provides additional evidence that the early solar system rearranged itself hundreds of millions years after the first solids formed.

Acknowledgment

Simone Marchi (SM) started this project in 2008 while at Padua University. As his appreciation of the knowledge and numerical subtlety needed to bring this project to fruition grew, so did the authorship list. Between 2008 and 2012, not only did new lunar data become available from LRO, but also SM moved to different institutes (OCA in Nice first, then NASA's Lunar Science Institute in Boulder, CO). During this time, SM prepared multiple drafts of this manuscript, each one reviewed, de-assembled, and put back together in a stronger form as he and his co-authors learned more and more about cratering processes and the Moon itself. In total, this work took advantage of untold numbers of discussions with crater and lunar experts. We wish to thank all of them for their criticisms and positive comments that made this document what it is today. In particular, we wish to thank our three EPSL reviewers: N. G. Barlow; N. Artemieva and G. Collins. The contributions of SM, W. F. Bottke, and D. A. Kring were supported by the NASA Lunar Science Institute (Center for Lunar Origin and Evolution at the Southwest Research Institute in Boulder, CO - NASA Grant NNA09DB32A; Center for Lunar Science and Exploration at the Lunar and Planetary Institute in Houston, TX). A. Morbidelli and SM are grateful to the Helmholtz Alliance "Planetary Evolution and Life" for support. This is LPI Contribution No. 1655.

Appendix A. Supplementary data

Supplementary data to this article can be found online at doi:10.1016/j.epsl.2012.01.021.

References

Bottke, W.F., Chapman, C.R., 2006. 37th Annual Lunar and Planetary Science Conference, 37, p. 1349.
Bottke, W.F., Durda, D.D., Nesvorný, D., Jedicke, R., Morbidelli, A., Vokrouhlický, D., Levison, H.F., 2005. Icarus 179, 63.
Bottke, W.F., Levison, H.F., Nesvorný, D., Dones, L., 2007. Icarus 190, 203.
Bottke et al., Nature, submitted for publication.
Chapman, C.R., McKinnon, W.B., 1986. IAU Colloq. 77: Some Background about Satellites, 492.
Chapman, C.R., Cohen, B.A., Grinspoon, D.H., 2007. Icarus 189, 233.
Cohen, B.A., Swindle, T.D., Kring, D.A., 2000. Science 290, 1754.
Crater Analysis Techniques Working GroupArvidson, R.E., Boyce, J., et al., 1979. Icarus 37, 467.
Elkins-Tanton, L.T., Burgess, S., Yin, Q.-Z., 2011. Earth Planet. Sci. Lett. 304, 326.
Elston, D.P., 1972. USGS Geologic map of the Colombo quadrangle (I-714).
Gault, D.E., 1970. Radio Sci. 5, 273.
Gibson, K.E., Jolliff, B.L., 2011. Lunar and Planetary Institute Science Conference Abstracts, 42, p. 2326.
Gomes, R., Levison, H.F., Tsiganis, K., Morbidelli, A., 2005. Nature 435, 466–469.
Hartmann, W.K., 1975. Icarus 24, 181.
Hartmann, W.K., et al., 1981. Chronology of Planetary Volcanism by Comparative Studies of Planetary Craters, Basaltic Volcanism on the Terrestrial Planets. Pergamon Press, Elmsford, NY, pp. 1050–1127.
Hartmann, W.K., Quantin, C., Mangold, N., 2007. Icarus 186, 11.
Haskin, L.A., Korotev, R.L., Rockow, K.M., Jolliff, B.L., 1998. Meteorit. Planet. Sci. 33, 959.
Head, J.W., Fassett, C.I., Kadish, S.J., Smith, D.E., Zuber, M.T., Neumann, G.A., Mazarico, E., 2010. Science 329, 1504.
Hodges, C.A., 1973. USGS Geologic map of the Langrenus quadrangle (I-739).
Ivanov, B.A., 2006. Icarus 183, 504.
Kring, D.A., Cohen, B.A., 2002. J. Geophys. Res. Planets 107, 5009.
Marchi, S., Mottola, S., Cremonese, G., Massironi, M., Martellato, E., 2009. Astron. J. 137, 4936.
McGetchin, T.R., Settle, M., Head, J.W., 1973. Earth Planet. Sci. Lett. 20, 226.
Milton, D.J., 1968. USGS Geologic map of the Theophilus quadrangle (I-546).
Minton, D.A., Malhotra, R., 2009. Nature 457, 1109.
Minton, D.A., Malhotra, R., 2010. Icarus 207, 744.
Morbidelli, A., Vokrouhlický, D., 2003. Icarus 163, 120.
Morbidelli, A., Petit, J.-M., Gladman, B., Chambers, J., 2001. Meteorit. Planet. Sci. 36, 371.

Neukum, G., Ivanov, B.A., 1994. Hazards Due to Comets and Asteroids. p. 359.
Norman, M.D., Duncan, R.A., Huard, J.J., 2010. Geochim. Cosmochim. Acta 74, 763–783.
Richardson, J.E., 2009. Icarus 204, 697.
Rowan, L.C., 1971. USGS Geologic map of the Rupes Altai quadrangle (I-690).
Ryder, G., 2002. J. Geophys. Res. Planets 107, 5022.
Schmidt, R.M., Housen, K.R., 1987. Int. J. Impact Eng. 5, 543.
Smith, D.E., et al., 2010. J. Geophys. Res. 37, 18204.
Stöffler, D., Ryder, G., 2001. Space Sci. Rev. 96, 9.
Strom, R.G., 1977. Phys. Earth Planet. Inter. 15, 156.
Strom, R.G., Neukum, G., 1988. Mercury. University of Arizona Press, p. 336.
Strom, R.G., Malhotra, R., Ito, T., Yoshida, F., Kring, D.A., 2005. Science 309, 1847.
Stuart-Alexander, D.E., Tabor, R.W., 1972. USGS Geologic map of the Fracastorius quadrangle (I-720).
Tera, F., Papanastassiou, D.A., Wasserburg, G.J., 1974. Earth Planet. Sci. Lett. 22, 1.
Turner, G., Cadogan, P.H., Yonge, C.J., 1973. Proc. Fourth Lunar Sci. Conf. pp. 1889–1914.
Walsh, K.J., Morbidelli, A., Raymond, S.N., O'Brien, D.P., Mandell, A.M., 2011. Nature 475, 206.
Wetherill, G.W., 1977. Meteoritics 12, 387.
Wilhelms, D.E., 1987. The Geologic History of the Moon. (U.S. Geol. Surv. Prof. Pap. 1348).
Wilhelms, D.E., Oberbeck, V.R., Aggarwal, H.R., 1978. Lunar and Planetary Science Conference Proceedings, 9, p. 3735.
Woronow, A., 1985. J. Geophys. Res. 90, 817.